THE JOURNAL OF BIOLOGICAL CHEMISTRY VOL. 285, NO. 7, pp. 4896–4908, February 12, 2010

Differential Functions of ApoER2 and Very Low Density Lipoprotein Receptor in Reelin Signaling Depend on Differential Sorting of the Receptors*[S]

Received for publication, May 27, 2009, and in revised form, October 27, 2009 Published, JBC Papers in Press, November 29, 2009, DOI 10.1074/jbc.M109.025973

Sarah Duit, Harald Mayer, Sophia M. Blake, Wolfgang J. Schneider, and Johannes Nimpf[1]

From the Max F. Perutz Laboratories, University Departments at the Vienna Biocenter, Department of Medical Biochemistry, Medical University of Vienna, Dr. Bohrgasse 9/2, A-1030 Vienna, Austria

ApoER2 and very low density lipoprotein (VLDL) receptor transmit the Reelin signal into target cells of the central nervous system. To a certain extent, both receptors can compensate for each other, and only the loss of both receptors results in the *reeler* phenotype, which is characterized by a gross defect in the architecture of laminated brain structures. Nevertheless, both receptors also have specific distinct functions, as corroborated by analyses of the subtle phenotypes displayed in mice lacking either ApoER2 or VLDL receptor. The differences in their function(s), however, have not been defined at the cellular level. Here, using a panel of chimeric receptors, we demonstrate that endocytosis of Reelin and the fate of the individual receptors upon stimulation are linked to their specific sorting to raft *versus* non-raft domains of the plasma membrane. VLDL receptor residing in the non-raft domain endocytoses and destines Reelin for degradation via the clathrin-coated pit/clathrin-coated vesicle/endosome pathway without being degraded to a significant extent. Binding of Reelin to ApoER2, a resident of rafts, leads to the production of specific receptor fragments with specific functions of their own and to degradation of ApoER2 via lysosomes. These features contribute to a receptor-specific fine tuning of the Reelin signal, leading to a novel model that emphasizes negative feedback loops specifically mediated by ApoER2 and VLDL receptor, respectively.

Defective Reelin signaling causes lamination defects in many areas of the cerebral cortex, hippocampus, and cerebellum (1, 2). The major abnormality in the cortex arises during embryogenesis from the inability of radially migrating neurons to invade and split the preplate. These neurons settle beneath the preplate, which is shifted toward the pial surface, where it forms a "superplate" in affected animals. Consequently, later born neurons cannot bypass earlier neurons that have settled beneath the superplate so that consecutive waves of neurons generated in the subventricular zone and migrating outwards establish a pattern of inverted neuronal layers. The role of Reelin in the correct lamination of certain brain structures was recently compiled in the "detach and go" model (3), where Reelin was proposed to promote detachment of migrating neurons from glial fibers and their translocation to the outermost area of the developing cortical plate. Despite recent progress in understanding molecular events in the Reelin signaling pathway (reviewed in Refs. 4 and 5), our knowledge about the modulation of the initial signal and downstream events guiding migration and positioning of neurons or modulating other processes like dendrite development is still scarce (6, 7). Proposed mechanisms involve Lis1 (8), Nckβ (9), and differential modulation of phosphatidylinositol 3-kinase-downstream pathways employing mTOR or GSK3β (10). The key events indispensable for triggering these pathways are binding of Reelin to ApoER2 and VLDL[2] receptor (VLDLR) and subsequent phosphorylation of Dab1. Obviously, Reelin-mediated receptor clustering triggers tyrosine phosphorylation of Dab1 (11). This event, however, does not seem to be sufficient to evoke the full Reelin signal, because anti-receptor antibodies that trigger Dab1 phosphorylation by receptor clustering do not rescue the *reeler* phenotype in brain slice cultures (12). In addition, thrombospondin 1, which is another functional ligand for ApoER2 and VLDLR in the brain, promotes Dab1 phosphorylation without eliciting the canonical Reelin signaling pathway (13).

Dab1 phosphorylation is mediated by members of the Src family of kinases (14–16). Mice lacking both Fyn and Src develop a phenotype similar to that of the Dab1-deficient scrambler mice (17). Dab1 binds to the NFDNP*X*Y sequence motif present in the cytosolic domains of ApoER2 and VLDLR (18). This domain is indispensable for Reelin signaling, since mice lacking VLDLR and carrying mutant alleles for ApoER2 coding for an altered NFDNPVY motif that does not bind Dab1 develop a *reeler* phenotype (19). This domain is also present in other members of the LDL receptor gene family, such as LDL receptor, LRP1, and LRP2 (20), and plays a key role in clathrin-mediated endocytosis of these receptors. In a Dab1-overexpressing cell model system, Dab1 decreases the endocytosis rate of the LDL receptor by interfering with the formation of the endo-

* This work was supported by the "Fonds zur Förderung der Wissenschaftlichen Forschung, FWF," Austria, Grants P16872-B09 and P19611-B09 and the Herzfelder'sche Familienstiftung.

[S] The on-line version of this article (available at http://www.jbc.org) contains supplemental Figs. 1–4.

[1] To whom correspondence should be addressed. Tel.: 43-1-4277-61808; Fax: 43-1-4277-9618; E-mail: johannes.nimpf@meduniwien.ac.at.

[2] The abbreviations used are: VLDL, very low density lipoprotein; VLDLR, VLDL receptor; MES, 4-morpholineethanesulfonic acid; DMEM, Dulbecco's modified Eagle's medium; RCM, Reelin conditioned medium; MCM, mock conditioned medium; Ab, antibody; HRP, horseradish peroxidase; IOD, integrated optical density; CLM, caveolin-rich light membrane(s); PBS, phosphate-buffered saline; CCV, clathrin-coated vesicle; NCM, non-caveolae membrane(s); CDX, methyl-β-cyclodextrin; CTF, C-terminal fragment; EEA1, early endosomal antigen 1.

cytosis complex (21). However, because Dab1 is brain-specific, the interaction with LDL receptor, LRP1, and LRP2 and the interference with endocytosis of these receptors most likely are not of physiological relevance. Our own studies and others have demonstrated that ApoER2 associates with lipid rafts, whereas VLDLR is strictly excluded from these microdomains (22–24). Despite its raft association, ApoER2 is endocytosed via the clathrin-mediated process, apparently through its association with Dab2 (22). It is still unclear, however, how important endocytosis of ApoER2 and VLDLR is in Reelin signaling.

With the identification of ApoER2 and VLDLR as functional Reelin receptors, it became evident that both receptors can compensate for each other to a certain extent, since only the lack of both receptors causes the *reeler* phenotype (25). Loss of ApoER2 or VLDLR alone causes subtle but distinguishable phenotypes, pointing to VLDLR being more important for the development of the cerebellum and ApoER2 for lamination of the cortex. This fact was recently corroborated by detailed studies on the divergent roles of ApoER2 and VLDLR in the migration of cortical neurons (26), which demonstrated that ApoER2 is indispensable for the correct migration of late generated neurons, whereas the VLDLR-mediated Reelin signal prevents neurons from entering the marginal zone.

Because both receptors mediate Dab1 phosphorylation, the question of the molecular substrate for their individual functions arises. Using chimeric receptor constructs and a fibroblast model system, we now demonstrate that endocytosis and cellular trafficking differ between ApoER2 and VLDLR and relate to raft *versus* non-raft localization of these receptors.

EXPERIMENTAL PROCEDURES

Cell Culture and Preparation of Conditioned Media—NIH 3T3 and 293 HEK cells were cultivated in Dulbecco's modified Eagle's medium (DMEM; Invitrogen) supplemented with 10% fetal calf serum (Invitrogen), and penicillin/streptomycin (Invitrogen) at 37 °C and 7.5% CO_2. Stable NIH 3T3-based cell lines expressing murine ApoER2 harboring LA repeats 1–3, 7, and 8 and containing the proline-rich cytoplasmic insert (3T3 A), murine VLDLR lacking the O-linked sugar domain (3T3 V), or either receptor and murine Dab1 (3T3 A/D and 3T3 V/D) (23) were kept under puromycin selection (0.75 μg/ml). Stable cell lines expressing chimeric receptors were generated as described for 3T3 A and 3T3 V (23) and were grown under the same conditions. 24 h before the experiment, puromycin-resistant cells were switched to growth medium lacking puromycin. Reelin-expressing 293 HEK cells were cultivated and used for production of Reelin conditioned medium (RCM) as described before (27). Mock conditioned medium (MCM) was prepared from untransfected 293 HEK cells using the same procedure. Primary rat neuronal cultures were obtained from embryonic day 16.5 rat embryonic brains and were kept in DMEM/F-12 (Invitrogen) containing B27 supplement (Invitrogen) and penicillin/streptomycin at 37 °C and 5% CO_2 for 72 h before use as described (11). Transient transfection of 3T3 was done using Lipofectamine 2000 (Invitrogen) according to the manufacturer's protocol.

Cloning of Chimeric Receptors—The following primers were used for generation of chimeric receptor constructs. VLDLR and ApoER2 primer pairs, spanning the respective full-length murine cDNAs, each containing an EcoRI restriction site (underlined), were as follows: VLDLR sense primer (primer 1) (5′-CGG AAT TCA TGG GCA CGT CCG CGC GC-3′), VLDLR antisense primer (primer 2) (5′-ATG AAT TCA AGC CAG ATC ATC ATC TGT GCT TAC-3′), ApoER2 sense primer (primer 3) (5′-ATG AAT TCA TGG GCC GCC CAG AAC TGG-3′), and ApoER2 antisense primer (primer 4) (5′-ATG AAT TCT CAG GGC AGT CCA TCA TCT TC-3′). ApoER2-VLDLR chimeric primers, annealing to ApoER2 at their 5′ region (shown in italic type) and to VLDLR at their 3′ region (underlined) were as follows: sense primer (primer 5) (5′-*GGT ACC TCA TCT GGA GGA A*TT GGC AAC-3′) and antisense primer (primer 6) (5′-*CGC TTC CAG TTC CTC CAC* ATC AAG TAG CC-3′), recognizing the junction of transmembrane and intracellular domain, and sense primer (primer 9) (5′-*CAA CAG TCA CCG CTG CTG* CTG CCT GGG-3′) and antisense primer (primer 10) (5′-*CCC AAT GAC* TGA AGT CCC TTT TGG GGG AAC-3′), recognizing the junction of extracellular and transmembrane domain. VLDLR-ApoER2 chimeric primers, annealing to VLDLR at their 5′ region (underlined) and to ApoER2 at their 3′ region (italic type) were as follows: sense primer (primer 7) (5′-GGC TAC TTG ATG *TGG AGG AAC TGG AAG CG*-3′) and antisense primer (primer 8) (5′-GTT GCC AAT *TCC TCC AGA TGA GGT AAC CAC*-3′), recognizing the junction of transmembrane and intracellular domain, and sense primer (primer 11) (5′-CCA AAA GGG ACT TCA *GTC ATT GGG GTC ATC GTG C*-3′) and antisense primer (primer 12) (5′-GAT GGC CCA GGC AG*C AGC AGC GGT GAC TGT TGA GC*-3′), recognizing the junction of extracellular and transmembrane domain.

For the first round of PCR amplification, fragments of ApoER2 and VLDLR were amplified from pMSCVpuro-ApoER2 and pMSCVpuro-VLDLR (23), using the following primers: primers 1 and 10 for VLDLR extracellular domain, primers 3 and 12 for ApoER2 extracellular domain, primers 1 and 6 for VLDLR extracellular and transmembrane domain, primers 3 and 8 for ApoER2 extracellular and transmembrane domain, primers 9 and 2 for VLDLR transmembrane and intracellular domain, primers 11 and 4 for ApoER2 transmembrane and intracellular domain, primers 5 and 2 for VLDLR intracellular domain, and primers 7 and 4 for ApoER2 intracellular domain. The obtained fragments were purified and used as templates for another round of PCR amplification. Fragments harboring the VLDLR extracellular and transmembrane domain were mixed with fragments harboring the ApoER2 intracellular domain and *vice versa*, and fragments harboring the VLDLR extracellular domain were mixed with fragments harboring the ApoER2 transmembrane and intracellular domain and *vice versa*. Primers used for amplification were primers 1 and 4 for the VVA and VAA constructs and primers 3 and 2 for the AAV and AVV constructs. The PCR products obtained in this second PCR amplification step were cloned into the pMSCVpuro backbone using the EcoRI restriction site.

Antibodies—Antibodies against ApoER2 were Ab 186, raised against the entire ligand-binding domain (11); Ab 220, raised against the first ligand-binding repeat (28); and Ab 20, raised against the

cytoplasmic tail (29). The ligand-binding domain of VLDLR was detected using Ab 74, which was raised in rabbits using a maltose-binding protein fusion protein containing the first ligand binding repeat of VLDLR. Ab 187 (11) was used for detection of VLDLR in immunofluorescence assays. For immunoprecipitation of Dab1, Ab 48 and Ab 54 (11) against the short splice variant of murine Dab1 were used. Mouse anti-Dab1 (D4) and mouse anti-Reelin (G10) antibodies were kind gifts of Andre Goffinet (University of Louvain, Belgium). Mouse anti-Lis1 was obtained from Orly Reiner (Weizmann Institute of Science, Rehovot, Israel). The following antibodies were purchased from the indicated sources: mouse anti-VLDLR (6A6) and mouse anti-phosphotyrosine (PY99), Santa Cruz Biotechnology, Inc. (Santa Cruz, CA); mouse anti-HA (HA.11), Covance; mouse anti-clathrin heavy chain and rabbit anti-Caveolin, BD Transduction Laboratories; rabbit anti-early endosomal antigen 1, Affinity BioReagents; secondary HRP-conjugated anti-mouse and anti-rabbit antibodies, Jackson ImmunoResearch; Alexa Fluor 488 goat anti-mouse and Alexa Fluor 594 goat anti-rabbit, Molecular Probes.

Preparation of Cell Extracts, SDS-PAGE, and Western Blotting—Cells were washed twice with ice-cold PBS and lysed in Hunt buffer (20 mM Tris, pH 8.0, 100 mM NaCl, 0.5% Nonidet P-40, 1 mM EDTA) supplemented with proteinase inhibitor mix (Complete™, Roche Applied Science). Cell debris was removed by centrifugation for 5 min at 20,000 × *g*. Proteins were separated by reducing SDS-PAGE and transferred onto nitrocellulose membranes by semidry blotting. Membranes were blocked in PBS containing 0.1% Tween 20 and either 5% bovine serum albumin or 5% nonfat dry milk and incubated with primary and HRP-conjugated secondary antibodies. For detection, enhanced chemiluminescence solution (Pierce) was used. For quantification of Western blot results, integrated optical density (IOD) values of the bands were calculated using Gel-Pro analyzer software (Media Cybernetics) and normalized to IOD of the loading control. For ligand blots, cell extracts were separated by non-reducing SDS-PAGE and Western blotting, and membranes were blocked in TBS containing 5% bovine serum albumin and 2 mM $CaCl_2$ and incubated with RCM diluted with Opti-MEM (1:2) containing 2 mM $CaCl_2$ for 2 h before incubation with primary (G10) and secondary antibodies.

Reelin Uptake and Degradation Assay—NIH 3T3 cells expressing ApoER2 or VLDLR were precooled at 4 °C for 30 min and incubated with RCM at 4 °C for 1 h to allow for Reelin binding to the cells. After extensive washing with TBS, cells were covered with Opti-MEM (Invitrogen) and shifted to a 37 °C water bath. After the indicated periods, cell extracts were prepared using Hunt buffer and analyzed by Western blotting. Relative Reelin amounts were calculated from IOD values.

Dab1 Phosphorylation Assay—Cells expressing Dab1 and one of the receptors were starved for 1 h in plain DMEM and incubated for 1 h with RCM or MCM. Cell extracts were prepared in Hunt buffer containing protease inhibitor mix and phosphatase inhibitors (50 mM NaF and 2 mM Na_3VO_4) and used for immunoprecipitation. Extracts were incubated with anti-Dab1 antiserum overnight at 4 °C, 40 μl of a protein A-Sepharose bead slurry (Zymed Laboratories Inc.) were added, and samples were incubated for 1 h at 4 °C again. Beads were collected by centrifugation at 500 × *g* for 1 min and washed three times using Hunt buffer. Samples were analyzed by Western blotting.

Receptor Degradation and Fragmentation Assays—To analyze degradation and secretase-mediated fragmentation of ApoER2, receptor-expressing cells were starved for 1 h in plain DMEM or DMEM containing 20 μg/ml cycloheximide and incubated for 4 or 6 h with medium containing cycloheximide and the indicated ligands and supplements. Cell extracts were prepared in Hunt buffer and analyzed by Western blotting.

Isolation of Caveolin-rich Light Membranes (CLM)—CLM were prepared from stable NIH 3T3 fibroblasts grown to confluence in 15-cm dishes or from WT mouse embryonic brains isolated at embryonic day 15. All procedures were carried out at 4 °C. Briefly, cells were washed with TBS and pelleted by centrifugation (5 min, 1400 × *g*). The supernatant was removed, and cells were solubilized in TBS containing 2% Brij 78P (Fluka) and Complete™ protease inhibitors (Roche Applied Science) by passaging the cells 10 times through a 23-gauge needle. Cell debris was removed by centrifugation (10 min, 21,000 × *g*) and the lysate (0.6 ml) was mixed with 0.6 ml of 90% (w/v) sucrose in MBS (MES-buffered saline; 25 mM MES, pH 6.5, 150 mM NaCl) and transferred to an ultracentrifuge tube. A discontinuous sucrose gradient was formed above the homogenate by adding 2.5 ml of 35% (w/v) sucrose in MBS, followed by 0.6 ml of 5% (w/v) sucrose in MBS. After centrifugation at 160,000 × *g* for 20 h in a Beckman SW60Ti rotor at 4 °C, 0.44-ml fractions were collected from the top of the tube. Fraction 2 at the interface between the 5 and 35% sucrose boundaries was designated the CLM fraction.

Preparation of Clathrin-coated Vesicles—Coated vesicles were prepared from NIH 3T3 cells expressing either receptor grown to near confluence or primary rat neurons cultured for 72 h using a ^2H_2O, 8% sucrose gradient (30). Cells were washed twice with PBS and once with MES buffer (100 mM MES, pH 6.5, 1 mM EGTA, 0.5 mM $MgCl_2$, 3 mM NaN_3, Complete™ proteinase inhibitor mixture). All steps were carried out at 4 °C. Cells were scraped in MES buffer and homogenized using a Potter tissue grinder. The homogenate was centrifuged at 5000 × *g* for 5 min. The pellet was resuspended in MES buffer and centrifuged at 5000 × *g* for 5 min. The supernatants from the two centrifugations were combined and centrifuged at 100,000 × *g* for 60 min. The resulting pellet was resuspended in MES buffer and centrifuged at 10,000 × *g* for 10 min. The resulting pellet was resuspended in MES buffer again, and the centrifugation was repeated. The supernatants from the two centrifugation steps were combined and centrifuged at 100,000 × *g* for 60 min. The pellet was resuspended in 1 ml of MES buffer and centrifuged at 10,000 × *g* for 10 min; the resulting pellet was again resuspended using 1 ml of MES buffer and centrifuged at 10,000 × *g* for 10 min. The combined supernatants were loaded on the top of 2 ml of 8% sucrose in ^2H_2O and centrifuged at 80,000 × *g* for 2 h. The pellet, resuspended in MES buffer, was centrifuged at 20,000 × *g* for 10 min. The supernatant was recovered and designated as clathrin-coated vesicle (CCV) fraction. Protein concentration was determined using the Coomassie Plus protein assay reagent (Pierce) accord-

ing to the manufacturer's protocol, and equal protein amounts of cell lysates and CCV were subjected to SDS-PAGE and Western blotting.

Immunofluorescence Assays and Microscopy—Sterile glass coverslips were coated with 40 μg/ml poly-L-lysine in PBS for 1 h at room temperature. NIH 3T3 cells expressing ApoER2 or VLDLR were grown on the coverslips for 24 h using standard fibroblast growth medium. Cells were cooled to 4 °C, washed with ice-cold PBS, and overlaid with RCM. After 1 h of incubation, RCM was removed, and cells were washed and incubated with Opti-MEM at either 4 or 37 °C for 10 min. Subsequently, cells were washed and fixed with 4% paraformaldehyde fixative. Fixed cells were washed with PBS containing 100 mM glycine and incubated with 0.1% Triton X-100 in PBS for 2 min to permeabilize the plasma membrane. Cells were washed again with PBS, blocked for 30 min with blocking solution (1% bovine serum albumin in phosphate-buffered saline) at room temperature, and incubated with primary and secondary antibodies diluted in blocking solution for 1 h each. Coverslips were washed again and mounted on glass slides using DAKO fluorescent mounting medium (Dako Corp.). Slides were analyzed using a confocal fluorescence microscope (laser-scanning microscope 510, Zeiss) and the corresponding software (Zeiss LSM Image Browser). Antibodies used for detection were Ab 186 for ApoER2, Ab 187 for VLDLR, G10 for Reelin, anti-early endosomal antigen 1, and secondary Alexa Fluor-coupled anti-mouse and anti-rabbit antibodies.

RESULTS

Expression and Subcellular Sorting of Chimeric Receptors—We have recently demonstrated that (i) ApoER2 and VLDLR reside in distinct subdomains of the plasma membrane and (ii) independently of this localization, both receptors mediate Reelin-induced Dab1 phosphorylation (23). Thus, we reasoned that recently unraveled functional differences of ApoER2 and VLDLR in migration of cortical neurons (26) could be due to differences in ligand endocytosis and intracellular trafficking of the receptors. Such differences might be caused either by differential sorting of the receptors to raft *versus* non-raft domains or by intrinsic properties of the receptor molecules independent of their sorting. To distinguish between these possibilities, we constructed a panel of chimeric receptors by swapping the respective intracellular, transmembrane (*TM*), and extracellular domains as detailed in Fig. 1*A*. The resulting chimeric receptors termed VVA, AAV, VAA, and AVV (V, derived from VLDLR; A, derived from ApoER2; in the order from left to right: extracellular domain, transmembrane, cytoplasmic domain), were expressed in 3T3 mouse fibroblasts and tested for functionality. As demonstrated in supplemental Fig. 1*A*, all constructs were expressed at comparable levels and were recognized by the appropriate antibodies (corresponding epitopes for the antibodies used are indicated in Fig. 1*A*). The faint double band produced by Ab 74 in cells expressing constructs not containing the extracellular domain of VLDLR must be due to cross-reactivity with an unrelated protein because it is also present in mock-transfected 3T3 cells. Furthermore, all constructs containing the extracellular domain derived from ApoER2 produce a double band, which is characteristic for ApoER2 and represents the precursor and the mature form of the receptor (23). All chimeric receptors bind Reelin, as tested by ligand blotting (supplemental Fig. 1*B*), and 3T3 fibroblasts expressing Dab1 (23), and any one of the chimeric receptors respond to Reelin with robust Dab1 phosphorylation as the WT receptors do (supplemental Fig. 1*C*). Next, we compared the subcellular localization of the chimeras with those of the WT receptors by separating the cell membranes into CLM and heavy membrane fractions containing ER membranes and non-raft fractions of the plasma membrane (non-caveolae membranes (NCM)) as described (23). As demonstrated previously in fibroblasts (23), mature ApoER2 is predominantly present in the CLM fraction, characterized by the presence of caveolin, whereas the immature form of ApoER2 (present in the ER) and VLDLR are exclusively found in the heavy non-raft membrane fraction (Fig. 1*B*). This particular subcellular distribution is not a specific effect seen in fibroblasts but is also evident *in vivo* because the receptors follow the same distribution in membranes prepared from embryonic mouse brain (Fig. 1*C*). As demonstrated in Fig. 1*B*, chimeras expressed in fibroblasts and comprising the extracellular domain of VLDLR (VVA, VAA) are found in the NCM. In contrast, chimeras containing the extracellular domain of ApoER2 (AAV, AVV) follow the distribution of WT ApoER2 independently of the composition of the remaining parts of the receptors. Thus, the extracellular domain of ApoER2 determines its sorting to raft domains of the cell membrane.

This model system provides us with the opportunity to test whether Reelin endocytosis, receptor degradation, or specific receptor cleavage are determined by (i) specific molecular features of the respective intracellular domains of the receptors or (ii) their localization to raft or non-raft domains of the cell membrane.

Endocytosis—To evaluate the efficiency of ApoER2 and VLDLR to endocytose and degrade Reelin, we used fibroblast cell lines engineered to express selected components of the Reelin signaling pathway (23). The cells (3T3 V; 3T3 A) were incubated with Reelin at 4 °C to allow binding of the ligand. After washing the cells, Reelin-free medium was added, the cells were shifted to 37 °C, and at the indicated time points, cell-associated Reelin was measured by Western blotting using antibody G10, which interacts with full-length Reelin and the proteolytic fragments NR6 and NR2 (see supplemental Fig. 2). Because endocytosis and degradation of full-length Reelin and both fragments follow a similar kinetic (supplemental Fig. 2), only full-length Reelin is shown in the following figures. As demonstrated in Fig. 2, cells expressing VLDLR (3T3 V) degrade associated Reelin extremely quickly. After 12 min, more than 60%, and after 24 min, all of the detectable cell-associated Reelin was lost. In cells expressing ApoER2 (3T3 A), however, bound Reelin remained stably associated with the cells, slowly dropping to 75% of the starting level after 24 min of incubation at 37 °C (Fig. 2*B*). As control, we used the parental 3T3 cells not expressing any of the two receptors. These cells do not interact with Reelin, demonstrating that binding and subsequent loss of Reelin is dependent on the presence of the receptors. To test whether the effect is cell-specific, we transiently transfected HeLa cells with ApoER2 and VLDLR and

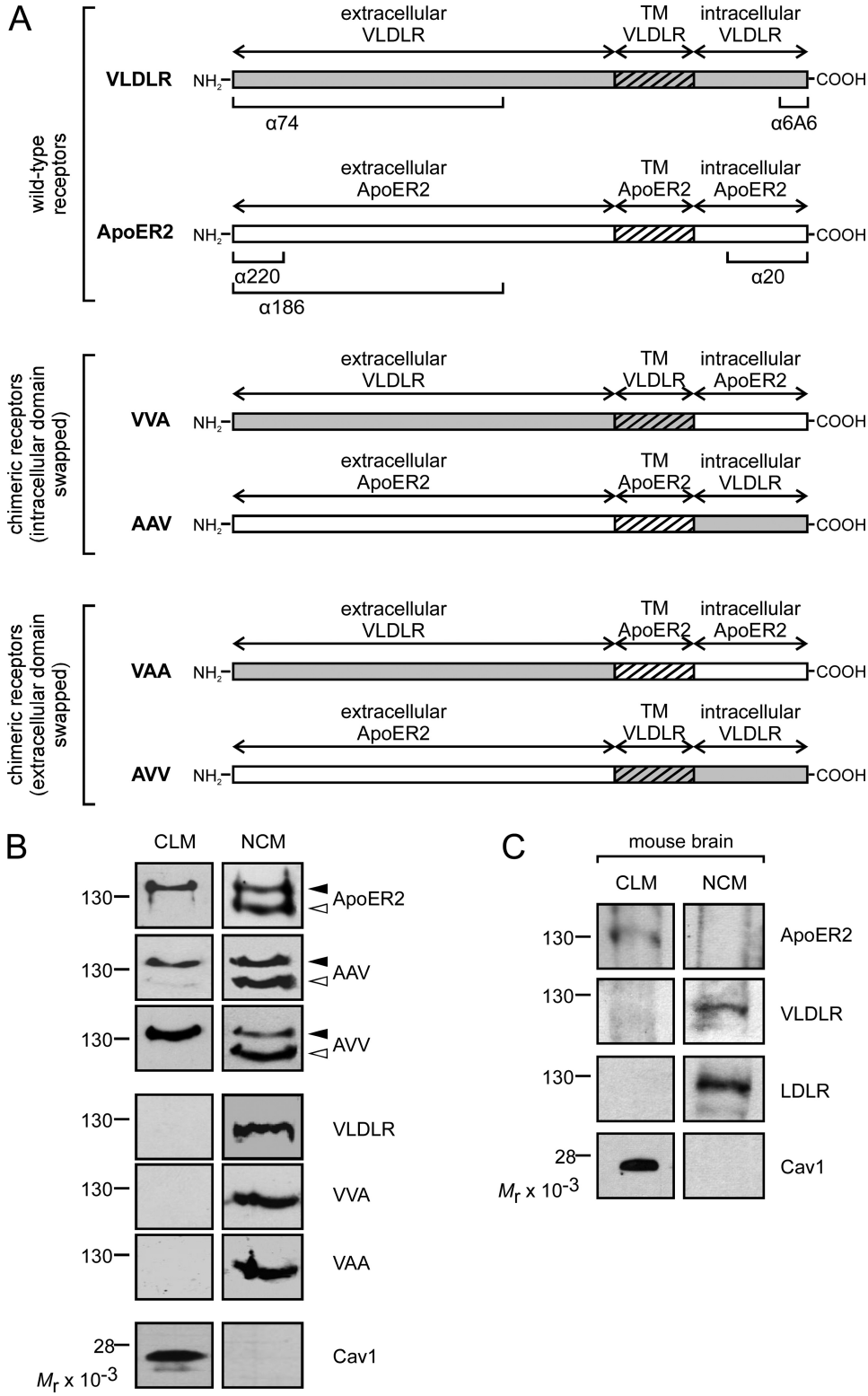

FIGURE 1. **Localization of ApoER2, VLDLR, and chimeric receptors within the plasma membrane.** *A*, schematic presentation of chimeric receptors consisting of intracellular, transmembrane (*TM*), and extracellular domains of ApoER2 (*A*) and VLDLR (*V*), respectively. Epitopes of the antibodies used are marked in the schematic diagram of the WT receptors. *B*, 3T3 cells expressing either of the receptors were fractionated by density centrifugation to prepare CLM and NCM fractions as described under "Experimental Procedures." The presence of the respective receptor was analyzed by Western blotting using Ab 20 for detection of ApoER2, VVA, and VAA and Ab 6A6 for detection of VLDLR, AAV, and AVV. *Filled* and *open arrows* indicate mature ApoER2, AAV, and AVV receptors and their unglycosylated precursors, respectively. The quality of the fractionation procedure was controlled by analyzing the presence of caveolin 1 by Western blotting using an anti-caveolin antibody. *C*, total brain extracts of embryonic WT mice (embryonic day 15; *E15*) were treated and analyzed as described above to detect the indicated proteins in CLM and NCM.

performed the same set of experiments. ApoER2- and VLDLR-mediated Reelin degradation followed the same kinetic as demonstrated for fibroblasts (data not shown). Thus, independent of cell type, VLDLR exhibits a high internalization rate leading to a fast removal of the ligand from the cell surface. In contrast, ApoER2, which resides in rafts, mediates very little Reelin degradation within the time frame relevant to Reelin signaling (20 min).

To evaluate whether Reelin is endocytosed by VLDLR and ApoER2 via the same intracellular pathway, we prepared CCVs from cell lysates and analyzed the content of this preparation by Western blotting. 3T3 cells expressing either ApoER2 or VLDLR and cultured primary neurons from WT rats were incubated in the presence of Reelin for 60 min and washed, and the CCVs were prepared and tested for the presence of the respective receptor and Reelin (Fig. 3). In 3T3 cells, Reelin and the corresponding receptor were always present in the CCV-enriched fraction, independent of the receptor expressed (Fig. 3*A*). Note that in CCV, only the mature form of ApoER2 is present, as expected. In primary neurons derived from WT rats that express VLDLR and ApoER2, Reelin and both receptors were present in the CCV preparation. In an alternative approach, we studied this process by immunofluorescence microscopy (Fig. 4). 3T3A and 3T3V cells were incubated at 4 °C with Reelin to allow receptor binding of the ligand in the absence of membrane-dependent endocytosis. Then the cells were incubated in Reelin-free medium for 10 min at 4 °C or 37 °C and fixed and processed for immunostaining with antibodies against Reelin, the respective receptor, and EEA1, respectively. As demonstrated in Fig. 4*A*, cells expressing ApoER2 or VLDLR incubated with Reelin at 4 °C exhibit prominent staining for Reelin outlining the cell surface. This staining is not continuous but shows a punctuate pattern that co-localizes with that obtained

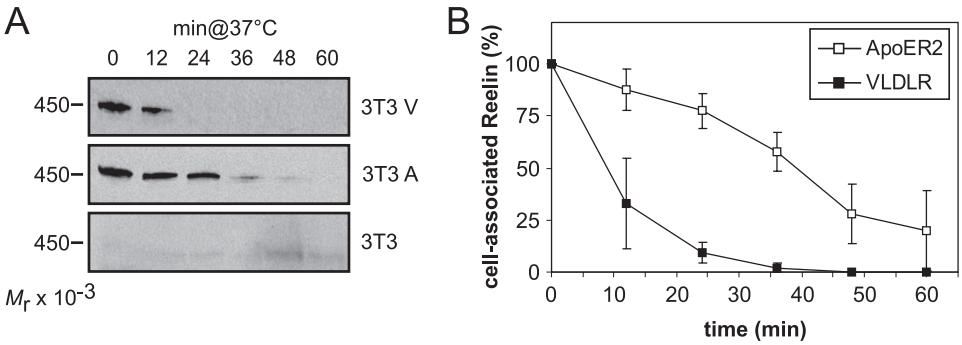

FIGURE 2. **VLDLR mediates Reelin endocytosis much more efficiently than ApoER2.** *A*, 3T3 cells expressing ApoER2 or VLDLR or mock-transfected 3T3 cells were incubated with RCM at 4 °C to allow binding of Reelin to the respective receptors. Cells were then shifted to 37 °C for the indicated time periods to allow internalization and degradation of the ligand. Extracts were prepared and analyzed for cell-associated Reelin by Western blotting using Ab G10 in combination with an HRP-coupled goat anti-mouse antibody. *B*, Western blots of *A* and two identical independent experiments were quantified by densitometry, and IOD values of the bands were normalized to the density of the band corresponding to the first time point. *Error bars*, S.E. ($n = 3$).

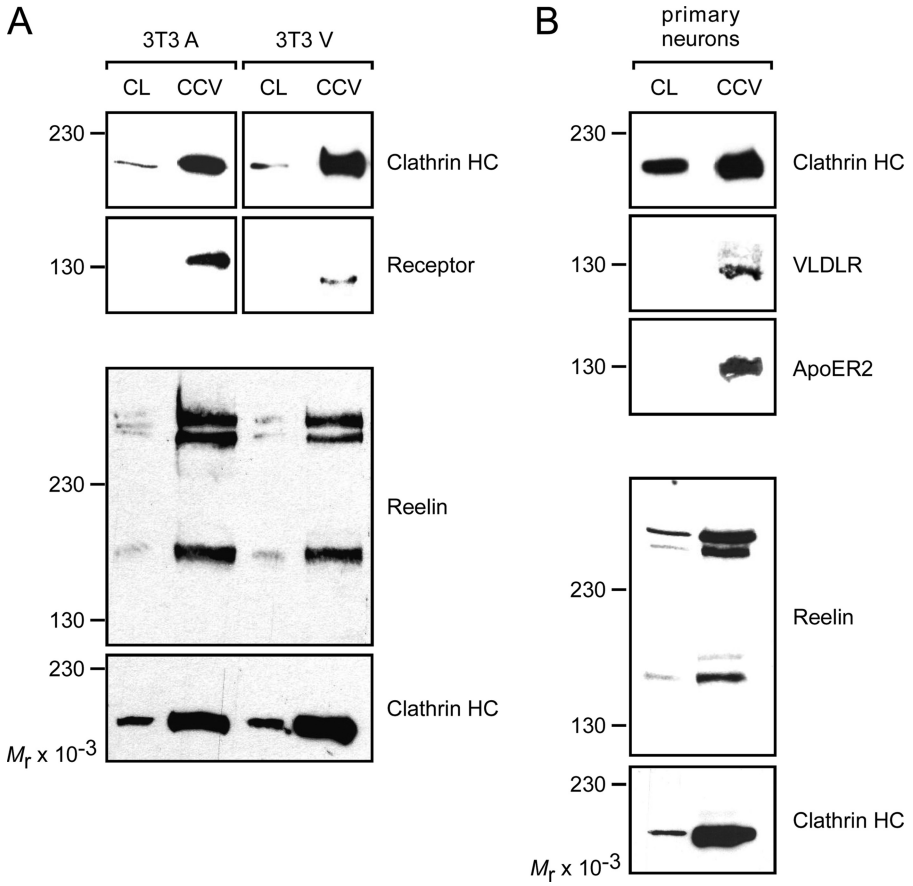

FIGURE 3. **ApoER2 and VLDLR internalize Reelin via clathrin-mediated endocytosis.** *A*, 3T3 cells expressing either ApoER2 or VLDLR were incubated with RCM for 1 h, and CCVs were prepared from total cell lysates (*CL*) as described under "Experimental Procedures." The presence of Reelin and the respective receptors was analyzed by Western blotting using the appropriate antibodies and the corresponding HRP-coupled secondary antibodies. Clathrin heavy chain was detected as control for enrichment of CCVs. *B*, CCVs were prepared from primary rat neurons and analyzed as described above.

with antibodies against the respective receptors. Under these conditions (endocytosis is blocked at 4 °C), Reelin does not co-localize with intracellular EEA1 (Fig. 4, *B* and *C*, 4 °C). After 10 min at 37 °C, Reelin appears in vesicular structures co-localizing with EEA1, independently of the receptor expressed. Together with the results obtained from the analysis of coated vesicles (Fig. 3), these data suggested that Reelin endocytosed via ApoER2 follows the same route as Reelin taken up by VLDLR (*i.e.* via clathrin-coated vesicles).

Having established that internalized ApoER2 and VLDLR follow the same pathway, we set out to investigate whether the different endocytosis rates for ApoER2 and VLDLR are due to their distinct membrane localization. Thus, internalization rates of Reelin were determined as performed for the WT receptors (Fig. 2) using cells expressing the different chimeric receptor constructs described in the legend to Fig. 1. As demonstrated in Fig. 5*A*, chimeric receptors containing the extracellular domain derived from ApoER2 exhibited the same endocytosis kinetics as WT ApoER2. The chimeras containing the extracellular domain of VLDLR, however, removed Reelin from the cell surface with the same rate as WT VLDLR (Fig. 5*B*). Thus, the receptor domains responsible for specific membrane localization of the receptors also determine their endocytosis rates. To test this notion further, cells expressing ApoER2 were treated with methyl-β-cyclodextrin (CDX), which removes cholesterol from the cell surface, thereby dissolving the raft structures. Because depletion of cholesterol also interferes with clathrin-mediated endocytosis (31), we determined the concentration of CDX (5 mM) that did not affect VLDLR-mediated Reelin endocytosis (data not shown). As previously reported (23), this treatment completely shifts ApoER2 into the non-raft fraction, and as demonstrated here (Fig. 5*C*), it increased the ApoER2-mediated Reelin endocytosis rate to that observed with VLDLR. These results demonstrate that the localization to rafts, rather than an intrinsic feature of the receptor, determines the slower endocytosis rate of ApoER2 in comparison with VLDLR.

Reelin-mediated Dab1 phosphorylation is necessary (32) but not sufficient to trigger the Reelin response in neurons (12). To test whether Reelin endocytosis is linked to or necessary for Dab1 phosphorylation, 3T3 cells expressing Dab1 and either ApoER2 or VLDLR (23) were exposed to Reelin at

37 or 4 °C. ApoER2 and VLDLR were both able to mediate Dab1 phosphorylation not only at 37 °C but importantly also at 4 °C (supplemental Fig. 3), demonstrating that Reelin endocytosis is not necessary for the primary signaling event.

Receptor Degradation and Processing—We have previously observed that in 3T3 cells expressing ApoER2, the receptor becomes dramatically down-regulated/degraded upon Reelin stimulation (23). To test whether the loss of ApoER2 is a specific feature of the 3T3 cell system and is mediated by the Reelin signaling cascade, we studied this effect in more detail. Primary rat neurons were stimulated for 5 h with Reelin, and the levels of ApoER2 and VLDLR were subsequently assessed by Western blotting (Fig. 6*A*, *lanes 1* and *4*). This treatment resulted in a significant loss of ApoER2, whereas VLDLR levels remained unchanged when compared with treatment with mock medium. Next, neurons and 3T3A cells were treated with Ab 186, which targets the extracellular domain of ApoER2 (see Fig. 1*A*) and induces Dab1 phosphorylation via receptor-clustering (23). As demonstrated in Fig. 6, *A* (*lane 3*; neurons) and *B* (*lane 2*; 3T3), treatment with Ab 186 also led to a dramatic loss of ApoER2. The effect of this antibody is specific because it could be blocked by the addition of soluble receptor fragment (Fig. 6*B*, *lane 3*, *MBP-ApoER2*), and an antibody against the intracellular domain of ApoER2 (Ab 20) had no effect (Fig. 6*B*, *lane 1*). The addition of receptor-associated protein, which binds to the receptors without inducing clustering and Dab1 phosphorylation had no effect (Fig. 6*B*, *lane 4*). These findings indicate that the loss of ApoER2 is mediated by receptor clustering and not merely by ligand binding and is a specific feature of ApoER2 but not of VLDLR. To test whether Reelin-mediated degradation of ApoER2 occurs via the lysosomal or the proteasomal pathway, we used specific inhibitors. The

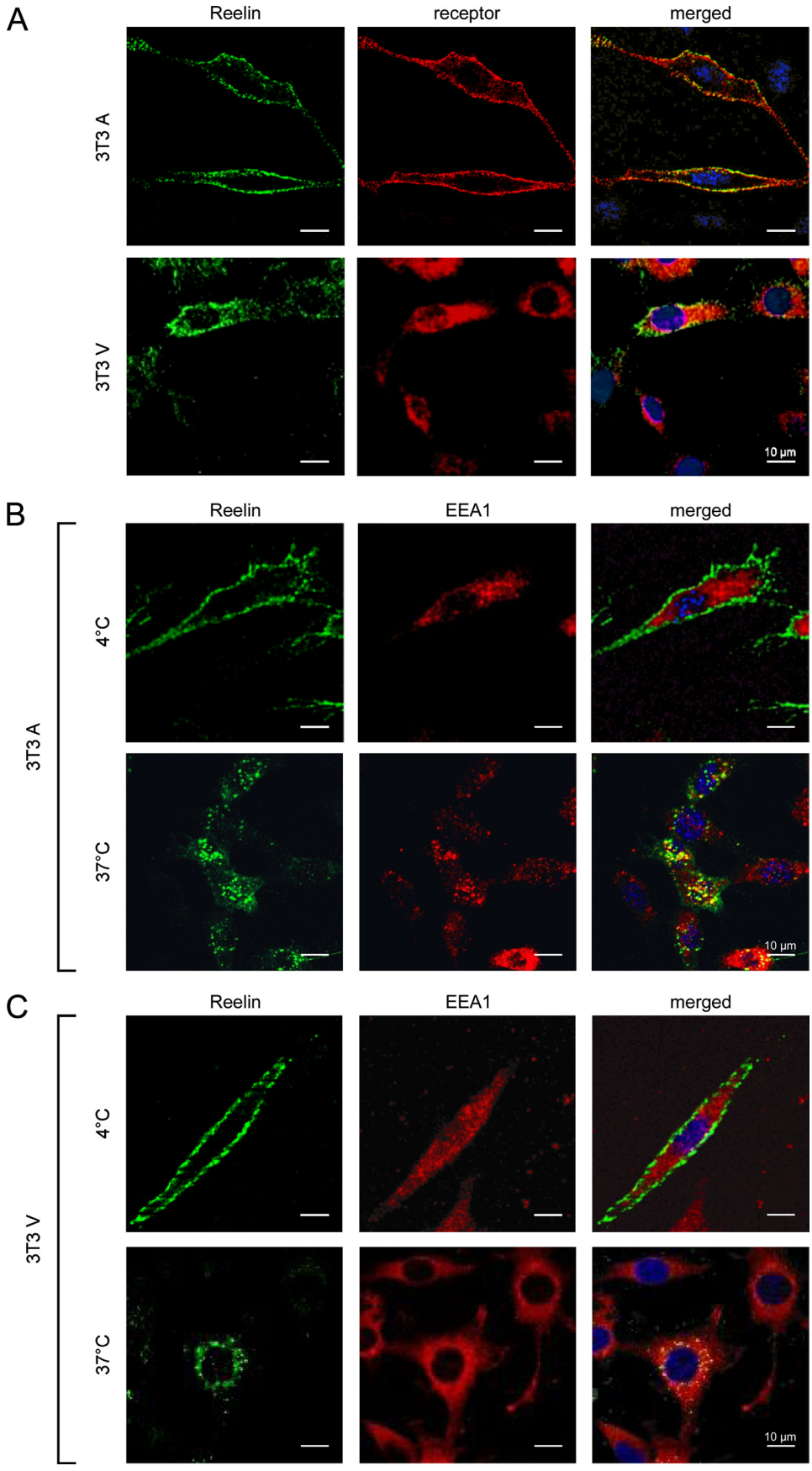

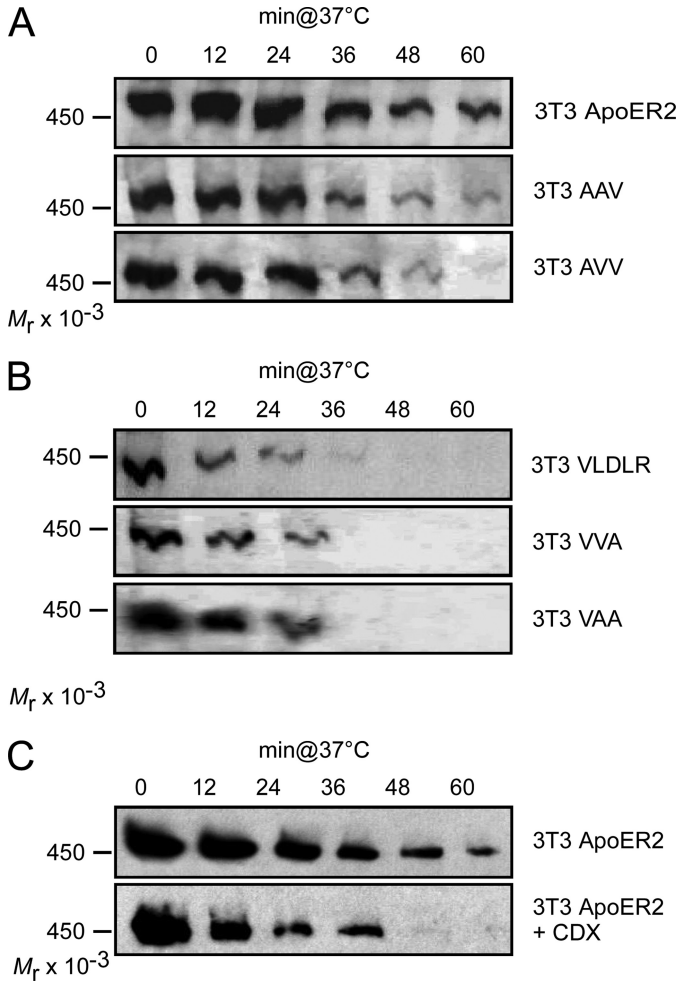

FIGURE 5. **Reelin internalization and degradation rates of ApoER2 and VLDLR depend on their sorting within the plasma membrane.** 3T3 cells expressing ApoER2 or one of the chimeric receptors containing the extracellular domain of ApoER2 (*A*) or VLDLR or one of the chimeric receptors containing the extracellular domain of VLDLR (*B*) were incubated with RCM at 4 °C to allow binding of Reelin to the respective receptors. Cells were then shifted to 37 °C for the indicated time periods to allow internalization and degradation of the ligand. After washing the cells, extracts were prepared and analyzed for cell-associated Reelin by Western blotting using Ab G10 in combination with an HRP-coupled goat anti-mouse antibody. *C*, 3T3 cells expressing ApoER2 were treated as described for *A* in the presence (*lower panel*) or absence (*upper panel*) of the raft-disrupting agent CDX (5 mM). Cell extracts were analyzed as described for *A*.

addition of the lysosomal blockers NH_4Cl and chloroquine reduced the degradation of ApoER2 (Fig. 6*C*), whereas MG132, an inhibitor of proteasomes, did not. From the results presented in Fig. 6 and those showing that ApoER2 is endocytosed via coated vesicles and early endosomes (Figs. 3 and 4), we conclude that ApoER2 is endocytosed via the coated pit/coated vesicle/endosome pathway and becomes degraded in the lysosome despite its localization in raft domains. Next, we evaluated the stability of the chimeric receptors. 3T3 cells expressing the individual chimeric receptors were treated with Reelin, and the fate of the receptors was evaluated by Western blotting. As demonstrated in Fig. 7*A*, all receptor variants containing the extracellular domain of ApoER2 became degraded upon Reelin stimulation, whereas variants containing the corresponding domain of VLDLR did not change their abundance. Reelin-induced degradation is not specific for raft-associated ApoER2, however, because raft-dissolving agents like CDX (Fig. 7*B*) or nystatin (Fig. 7*C*) did not inhibit this process.

Another aspect of the Reelin signaling cascade is the Reelin-induced cleavage of ApoER2, which produces a soluble extracellular (*NTF*) and a soluble intracellular fragment (intracellular domain; *ICD*) by the sequential action of α- and γ-secretase, respectively (33, 34) (Fig. 8*A*). Because the production of the intracellular domain cannot be monitored directly, most likely due to its inherent instability (34), we followed the production of the membrane-bound precursor CTF by Western blotting. Incubation of 3T3 cells expressing WT ApoER2 with Reelin resulted in a significant increase of the 25-kDa CTF (supplemental Fig. 4, *lane 1*), which was not observed upon the addition of receptor-associated protein (*lane 3*). Again, CTF production could be triggered by the bivalent agent Ab 186 (*lane 5*), and this was blocked by the addition of soluble receptor fragment (*lane 6*). For controls, the cells were incubated with mock-conditioned medium (*lane 2*) and Ab 20 (directed against the intracellular domain; *lane 4*). Under these conditions, small amounts of CTF were detected, apparently produced even when the cells are not stimulated. The properties of the chimeric receptors in regard to the specific fragmentation process (Fig. 8*B*) were more complex than those described above for receptor degradation and endocytosis. Although VLDLR does not undergo fragmentation at all (Fig. 8*C*, *lane 1*), chimeras containing the extracellular domain of ApoER2 produced significant amounts of CTF upon Reelin treatment (Fig. 8*C*, *lanes 3* and *5*). It should be noted that the antibody used (6A6) to detect the CTF containing the respective domains of VLDLR consistently gives weaker signals than Ab 20 directed against the intracellular domain of ApoER2. Chimeras containing the transmembrane plus intracellular domains (VAA) or only the intracellular domain of ApoER2 (VVA) are processed to a small extent, but this was not enhanced by Reelin (Fig. 8*B*, *lanes 3–6*). Disruption of rafts using CDX significantly blocked the Reelin-induced production of CTF from WT ApoER2 (Fig. 8*D*).

DISCUSSION

Inactivation of the genes for both Reelin receptors, ApoER2 and VLDLR, leads to a *reeler* phenotype in mice (25). Single knock-out mice lacking the gene either for ApoER2 or for VLDLR display only subtle abnormalities in their brain architectures. This suggests that ApoER2 and VLDLR can at least partially compensate for each other, at least in respect to their function in establishing laminated brain structures. This was confirmed in primary neurons and in a fibroblast cell model by

FIGURE 4. **ApoER2 and VLDLR internalize Reelin via the early endosomal compartment.** *A*, Reelin co-localizes with ApoER2 and VLDLR at 4 °C. 3T3 cells expressing ApoER2 (*upper panel*) or VLDLR (*lower panel*) were incubated with RCM at 4 °C to allow binding of Reelin to the receptors. Cells were fixed, permeabilized, and stained using Ab 186 for detection of ApoER2, Ab 187 for VLDLR, and Ab G10 for Reelin. *B* and *C*, internalized Reelin co-localizes with EEA1. 3T3 cells expressing ApoER2 (*B*) or VLDLR (*C*) were incubated with RCM at 4 °C for 1 h, washed, and incubated with Opti-MEM for 10 min at 4 °C (*upper panels*) or 37 °C (*lower panels*), respectively. Cells were fixed, permeabilized, and stained using Ab G10 for detection of Reelin and an antibody against EEA1 for staining of the early endosomal compartment. *Scale bars*, 10 μm.

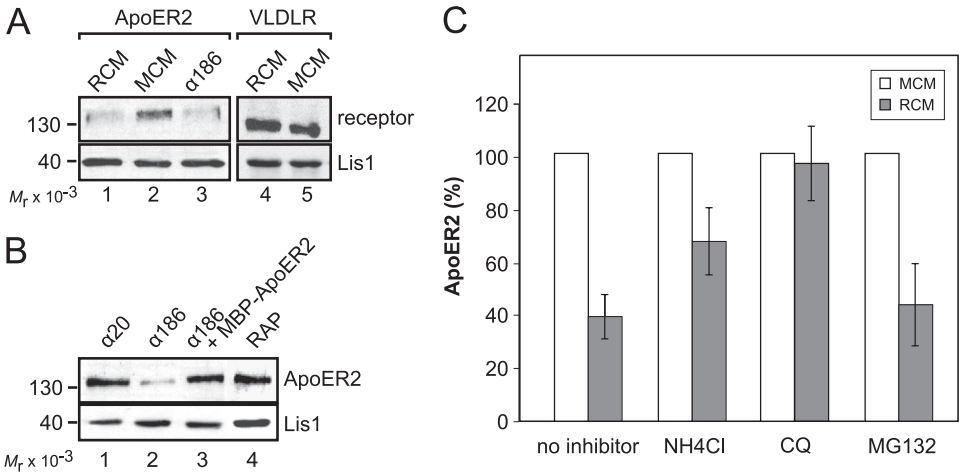

FIGURE 6. **ApoER2 degradation is induced by multivalent ligands and is mediated by the lysosomal pathway.** Primary rat neurons (*A*) and 3T3 cells expressing ApoER2 (*B*) were incubated for 5 h with RCM, MCM, Ab 186 (1:100; targets ApoER2 ligand binding domain), Ab 20 (1:100; targets ApoER2 intracellular domain), Ab 186 and recombinant ApoER2 N-terminal fragment *(MBP-ApoER2)*, or 20 μg/ml recombinant receptor-associated protein (*RAP*). Total cell extracts were analyzed by Western blotting using Ab 20 (ApoER2) and Ab 6A6 (VLDLR) and an antibody against Lis1 as a loading control in combination with the corresponding HRP-coupled secondary antibodies. *C*, ApoER2-expressing 3T3 cells were incubated with RCM or MCM. Lysosomal degradation was blocked by the addition of 10 mM NH4Cl or 25 μM chloroquine; proteasomal degradation was blocked using 25 μM MG132. Cell extracts were analyzed as described for *A* and *B*, and results were quantified by densitometry. IOD values of ApoER2 bands were normalized to the density of Lis1 bands. *Error bars*, S.E. ($n = 3$).

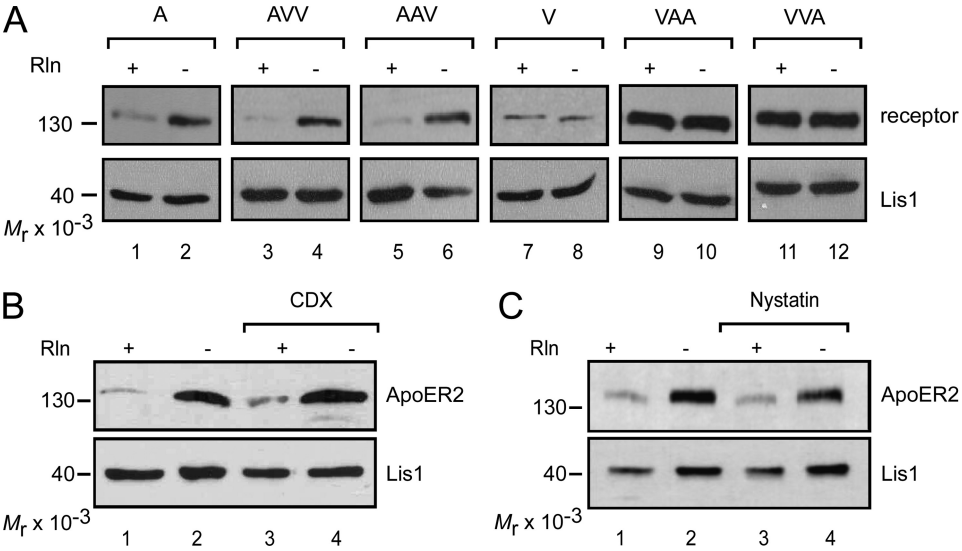

FIGURE 7. **The extracellular domain of ApoER2 but not its sorting to lipid rafts is required for Reelin-induced lysosomal receptor degradation.** *A*, 3T3 cells expressing one of the wild type (*A* and *V*) or chimeric receptors (*AVV*, *AAV*, *VAA*, and *VVA*) were stimulated with RCM (*lanes 1*, *3*, *5*, *7*, *9*, and *11*) or MCM (*lanes 2*, *4*, *6*, *8*, *10*, and *12*) for 5 h and analyzed for receptor degradation by Western blotting using Ab 20 for ApoER2, VAA, and VVA; Ab 220 for AAV and AVV; and Ab 74 for VLDLR. Lis1 was highlighted using an anti-Lis1 antibody and used as a loading control. *B*, ApoER2-expressing 3T3 fibroblasts were incubated with RCM (*lanes 1* and *3*) or MCM (*lanes 2* and *4*) and the raft-disrupting agent CDX (5 mM; *lanes 3* and *4*) for 5 h. Cell extracts were analyzed for ApoER2 degradation by Western blotting using Ab 20 in combination with an HRP-coupled goat-anti-rabbit antibody. Lis1 was highlighted using an anti-Lis1 antibody and used as a loading control. *C*, cells were treated and analyzed as described for *B*, except that 15 μg/ml nystatin was used for disruption of rafts.

demonstrating that the initial event of the Reelin signaling pathway (*i.e.* phosphorylation of Dab1) is equally well supported by ApoER2 and VLDLR (11, 23). Divergent roles for ApoER2 and VLDLR have been corroborated recently. In neuronal migration, VLDLR mediates a stop signal for migrating neurons, whereas ApoER2 plays a distinct role in the migration of neocortical neurons generated late (26). The specific phenotypes of the single knock-out animals and the observed distinct roles for both receptors might be in part caused by selective expression of the receptors in distinct areas of the brain (35). On the other hand, ApoER2 and VLDLR may have distinct functions in the Reelin pathway, apart from the primary phosphorylation event. Other processes in the central nervous system seem to depend on specific variants of ApoER2 only and involve the modulation of synaptic plasticity and memory (36), the control of neuronal survival (37), and selenium uptake (38, 39). One reason for differential functions of these receptors is structural differences in the respective intracellular domains (40) linking ApoER2 to adapters that do not interact with VLDLR (41). Other features could be selective expression in distinct subdomains of the cell membrane and/or their divergent endocytic competence. As shown in our laboratory, ApoER2 is prevalently present in raft domains, whereas VLDLR is not (23). The avian ortholog of VLDLR is expressed on growing oocytes where it efficiently mediates receptor-mediated endocytosis of yolk precursors, thus playing a pivotal role in follicle development (42), whereas ApoER2 was demonstrated to exert an extremely slow endocytosis rate in comparison with other members of the LDL receptor family (43). As recently postulated, VLDLR and/or ApoER2-mediated endocytosis of full-length Reelin or its central fragment produced by metalloproteinases might play an important role in the Reelin signaling pathway by controlling the strength of the signal via modulating the availability of the ligand (44). Thus, we set out to study structural features of the receptors that might be responsible for different fates and/or functions of the receptors in terms of cellular sorting, endocytosis, and receptor trafficking.

For most of the present studies, we used a recently established fibroblast-based cell system in which the Reelin signaling pathway has been partially reconstituted by expressing Dab1 and either ApoER2 or VLDLR (23). These cells respond to Reelin stimulation with Dab1 phosphorylation and phosphatidylinositol 3-kinase activation, leading to protein kinase B/Akt phosphorylation undistinguishable from primary neurons. In

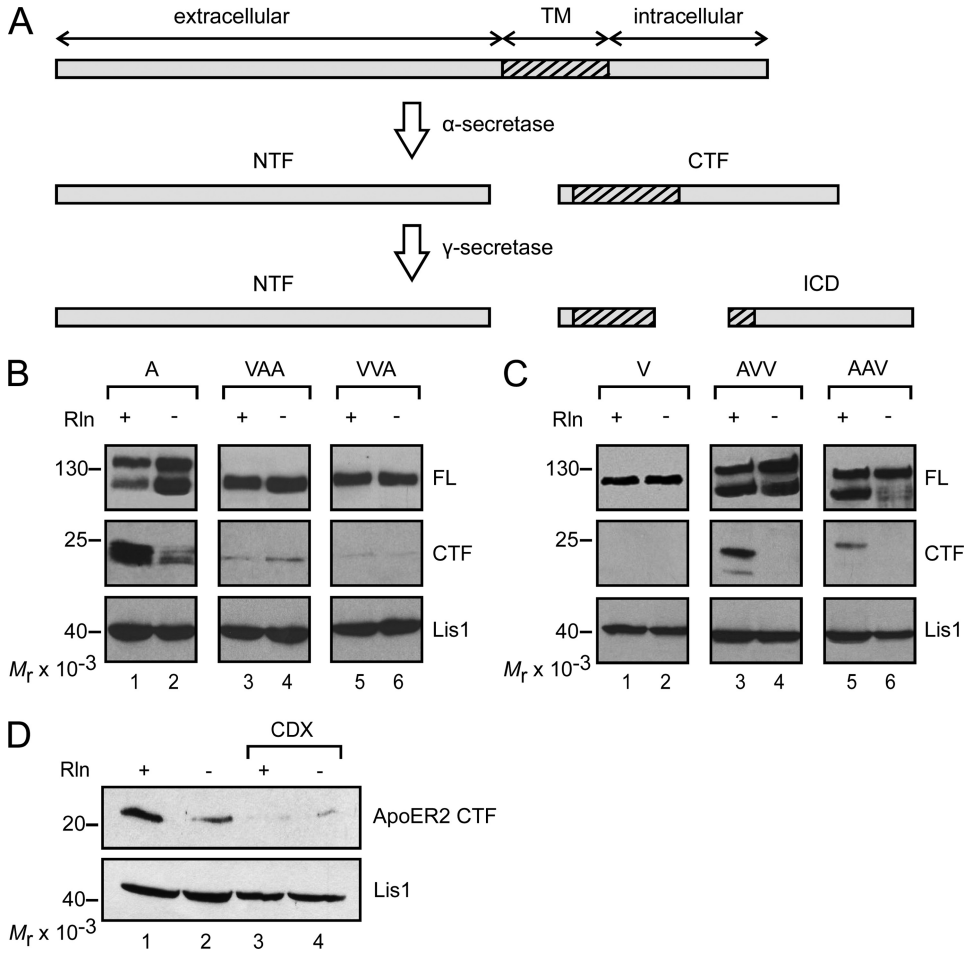

FIGURE 8. **Secretase-mediated cleavage of ApoER2 depends on the sorting of the receptor to lipid rafts.** *A*, ApoER2 is subjected to cleavage by α-secretase upon Reelin stimulation, thereby producing a soluble extracellular *N*-terminal fragment (*NTF*) and a membrane-bound C-terminal fragment (*CTF*). The latter is further processed by α-secretase to release a soluble intracellular domain (*ICD*). *B* and *C*, 3T3 fibroblasts expressing one of the WT (*A* and *V*) or chimeric receptors (*VAA*, *VVA*, *AVV*, and *AAV*) were stimulated with RCM or MCM. Cell extracts were analyzed by Western blotting using Ab 20 for detection of the CTF derived from A, VAA, and VVA (*B*) and Ab 6A6 for the CTF derived from V, AVV, and AAV (*C*). *D*, 3T3 cells expressing ApoER2 were treated as described for *B* and *C* in the presence (*lanes 3* and *4*) or absence (*lanes 1* and *2*) of CDX. Production of the CTF was analyzed as described for *B*. Lis1 was highlighted using an anti-Lis1 antibody and used as a loading control. *FL*, full-length.

addition, we have now used a panel of genetically engineered receptor chimeras between ApoER2 and VLDLR (Fig. 1*A*) to define the structural elements in the receptors responsible for differential sorting of the receptors. These chimeric receptors were also used to determine whether functional differences are caused by selective expression in raft *versus* non-raft domains or by intrinsic structural differences of the respective receptors.

As previously demonstrated by analysis of whole cell extracts (23), ApoER2 migrates as a distinct double band representing the precursor (lower band) and the fully glycosylated mature form (upper band), which is present in the raft domains of the plasma membrane. Expression of the chimeric receptors corroborates these findings, as the extracellular part of ApoER2 containing the *O*-linked sugar domain (45) directs the receptors to the raft fraction, whereas all constructs containing the extracellular domain of VLDLR did not show this behavior (Fig. 1*B*). Ligand blotting and evaluation of Reelin-induced and receptor-mediated Dab1 phosphorylation demonstrated that all chimeric receptor constructs are Reelin binding-competent (supplemental Fig. 1*B*) and transmit the signal into the cells equally well (supplemental Fig. 1*C*). Membrane fractionation studies allowed us to identify the extracellular domain of ApoER2 as the one responsible for directing the receptor to caveolae/rafts. This is reminiscent of epidermal growth factor receptor, which is also sorted to rafts; there, the responsible region was identified to be within 60 amino acids of the extracellular domain juxtaposed to the cell membrane representing the *O*-linked sugar domain (46). As reported in the same paper, glycosylation of this domain is indeed the key to such sorting, since when glycosylation is blocked, epidermal growth factor receptor is targeted to non-raft membrane domains. This is an interesting observation, because the predominant variant of VLDLR expressed in the brain lacks exactly this domain and is absent from the raft fraction (23). The fact that the sorting signal derives from the extracellular domain of the receptors allowed us to dissect whether specific functions of the receptors are due to their differential sorting or to structural differences in their respective intracellular domains.

The major finding of these studies is that VLDLR indeed internalizes Reelin very efficiently, resulting in a local depletion of Reelin. ApoER2, in contrast, endocytoses Reelin with very low efficiency, and cells expressing ApoER2 do not significantly decrease the concentration of Reelin in the medium. Although localized in the raft fraction of the plasma membrane, slow endocytosis of ApoER2 takes place via the classic endocytosis pathway involving coated pits/coated vesicles/early endosomes (Figs. 3 and 4). This is in agreement with previous findings demonstrating that ApoER2 is endocytosed independent of its raft association by a clathrin-mediated process involving the adapter Dab2 (22). It was demonstrated that the central fragment (R3-6) is critical to exert the signaling function of Reelin, suggesting that this domain of Reelin interacts with ApoER2 and VLDLR (12). The presence of NR2, which lacks the central part of Reelin (R3-6), in coated vesicles suggests that this fragment either stays associated with full-length Reelin via the oligomerization domain present in the N-terminal region (47) or that NR2 is produced after endocytosis. Using the panel of chimeric receptors and raft-dissolving agents like CDX, we demonstrate that it is the raft association of ApoER2 that causes its slow endocytosis rate. As soon as

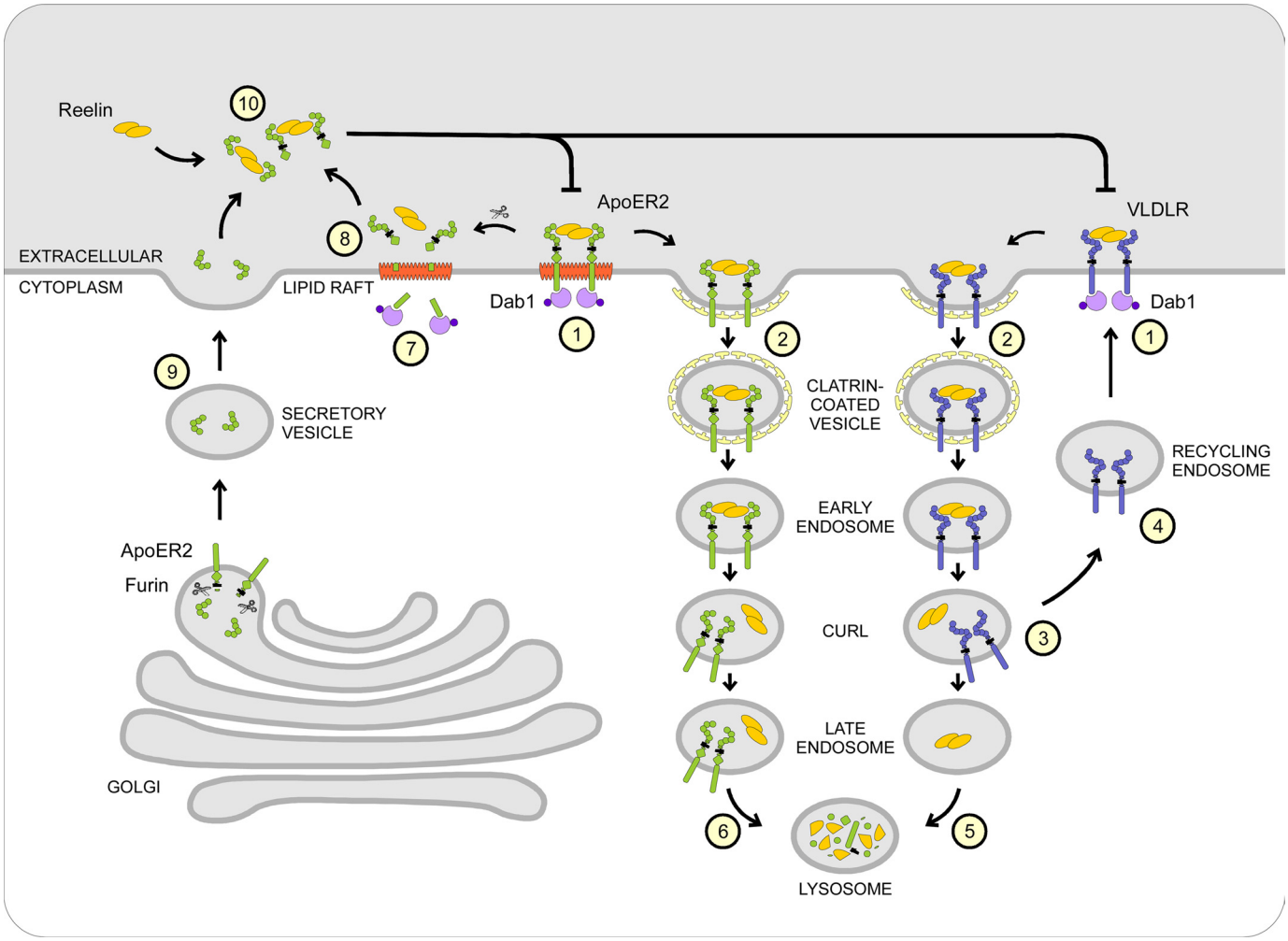

FIGURE 9. **Model of the intracellular fates of ApoER2 and VLDLR upon Reelin stimulation.** Upon binding of Reelin, both ApoER2 and VLDLR mediate phosphorylation of Dab1 (*step 1*). VLDLR internalizes Reelin rapidly via clathrin-mediated endocytosis (*step 2*) and is separated from Reelin in the compartment of uncoupling of receptor and ligand (*step 3*). VLDLR then recycles back to the plasma membrane (*step 4*), whereas Reelin is delivered to the lysosome for degradation (*step 5*). ApoER2 internalizes Reelin via the same pathway (*step 2*), although the receptor originally resides in lipid rafts and endocytoses its ligand at a much slower rate. In contrast to VLDLR, ApoER2 is not recycled but ends up in the lysosome together with Reelin (*step 6*). As an additional feedback mechanism, Reelin stimulation induces secretase-mediated cleavage of ApoER2, thereby generating a soluble intracellular fragment (ICD) (*step 7*), the function of which is not defined yet, and a soluble extracellular fragment containing the ligand binding domain (*step 8*). This fragment can, together with another N-terminal fragment produced from an ApoER2 isoform by furin cleavage (*step 9*), inhibit the Reelin signal by sequestering free Reelin in the surroundings of the cell (*step 10*).

ApoER2 loses its association with rafts, the endocytosis rate of the receptor increases significantly. This effect might even be underestimated by the experiment using CDX to dissolve the rafts because this agent also blocks clathrin-dependent endocytosis by generally depleting the membrane of cholesterol (31). Thus, slow translocation from rafts to non-raft domains of the membrane might be the rate-limiting step of ApoER2-mediated endocytosis.

The second significant difference between ApoER2 and VLDLR is the fact that the levels of ApoER2, but not of VLDLR, significantly drop in the presence of Reelin (23). As demonstrated here, Reelin-induced degradation of ApoER2 occurs via the lysosomal pathway and depends on the presence of receptor-clustering ligands. Again, the extracellular domain of ApoER2 determines the fate of the receptor upon binding of Reelin. Disruption of rafts by CDX or nystatin had no influence on receptor degradation, demonstrating that neither the caveolin-mediated pathway originating from raft structures nor the targeting of raft-associated receptors to endosomes (48) is responsible for receptor degradation. Thus, ApoER2 degradation most likely occurs by clathrin-mediated endocytosis and subsequent sorting to lysosomes. Structural differences in the extracellular domains of ApoER2 and VLDLR must be responsible for directing ApoER2 predominantly to lysosomes and VLDLR into the recycling pathway back to the plasma membrane. For the LDL receptor, it was shown that a distinct region of the extracellular domain (*i.e.* the cysteine-rich growth factor repeats (epidermal growth factor repeats)) is responsible for uncoupling of receptor and ligand within the endocytic pathway (49). When this domain is deleted, the receptor no longer releases its ligand and becomes degraded in the lysosome. Thus, we speculate that differences in the epidermal growth factor repeats between ApoER2 and VLDLR are responsible for the distinct behavior of the receptors.

Parallel to lysosomal degradation of ApoER2, specific breakdown products of this receptor are produced upon Reelin stim-

ulation (33, 34). Here we demonstrate that this effect (i) is not simply induced by binding of a ligand but requires the presence of a clustering ligand, such as Reelin, or antibodies against the extracellular domain, which also induce Dab1 phosphorylation; (ii) is dependent on the presence of the extracellular domain of ApoER2; and (iii) is dependent on the presence of rafts. VLDLR variants carrying the extracellular domain of ApoER2 are cleaved like ApoER2 itself, whereas intact VLDLR completely escapes this process. This is in agreement with previous findings that the presence of the *O*-linked sugar domain promotes γ-secretase-mediated cleavage of the receptor (34) and that the γ-secretase complex is associated with rafts (50, 51). Thus, most likely, the entire processing (α- and γ-secretase-mediated) takes place within the raft domain of the plasma membrane. Whether clustering of the receptors or Dab1 phosphorylation or both actually triggers the induction of the cleavage is still an open question.

These results allow us to propose a model for describing both the interrelated and independent functions of ApoER2 and VLDLR in Reelin signaling (Fig. 9). VLDLR present in non-raft domains of the plasma membrane binds Reelin, which results in Dab1 phosphorylation (Fig. 9, *step 1*). The Reelin-receptor complex is rapidly internalized by clathrin-mediated endocytosis (Fig. 9, *step 2*), and Reelin is uncoupled from the receptor (Fig. 9, *step 3*) and sorted to lysosomes (Fig. 9, *step 5*), whereas VLDLR recycles back to the cell membrane (Fig. 9, *step 4*). This reduces the amount of extracellular Reelin significantly, thus shutting off the persistence of the signal without rendering the cell refractory to VLDLR-mediated actions. Binding of Reelin to ApoER2 present in rafts also leads to immediate phosphorylation of Dab1 (Fig. 9, *step 1*) but not to a significant reduction of extracellular Reelin, because ApoER2-mediated endocytosis is slow. The Reelin signal itself can be turned off via degradation of phosphorylated Dab1, which occurs independently of the signaling receptor (52). Selective Reelin-mediated loss of ApoER2 depends on clathrin-mediated endocytosis and lysosomal degradation of the receptor (Fig. 9, *step 6*). As shown here, this process is much slower than for VLDLR but in the long run renders the target cell refractory to further Reelin stimulation until new receptor is synthesized. In parallel, specific fragmentation by α- and γ-secretases leads to the production of soluble intracellular receptor fragment (Fig. 9, *step 7*), which might exert its action within the nucleus (34), and a soluble extracellular fragment (Fig. 9, *step 8*). The extracellular fragment containing the ligand binding domain, together with secreted soluble ApoER2 fragments (Fig. 9, *step 9*) produced by the action of furin from certain splice variants of the receptor (28), bind Reelin and thereby attenuate the entire pathway (Fig. 9, *step 10*). Thus, in regions of the brain where mostly ApoER2 is expressed, the Reelin-induced activation of target cells is not accompanied by a reduction of Reelin. Thus, Reelin might keep exerting other functions without further inducing the canonical Reelin signal, which is efficiently turned off by Dab1 degradation and production of dominant negative receptor fragments. Whether the production of soluble intracellular fragments derived from ApoER2 by γ-secretase cleavage represents an independent signal within the cell as proposed (34) awaits clarification.

Acknowledgment—We appreciate the technical assistance of Harald Rumpler.

REFERENCES

1. Rice, D. S., Curran, T. (2001) *Annu. Rev. Neurosci.* **24,** 1005–1039
2. Lambert de Rouvroit, C., and Goffinet, A. M. (1998) *Adv. Anat. Embryol. Cell Biol.* **150,** 1–106
3. Cooper, J. A. (2008) *Trends Neurosci.* **31,** 113–119
4. Förster, E., Jossin, Y., Zhao, S., Chai, X., Frotscher, M., and Goffinet, A. M. (2006) *Eur. J. Neurosci.* **23,** 901–909
5. Tissir, F., and Goffinet, A. M. (2003) *Nat. Rev. Neurosci.* **4,** 496–505
6. Niu, S., Renfro, A., Quattrocchi, C. C., Sheldon, M., and D'Arcangelo, G. (2004) *Neuron* **41,** 71–84
7. Olson, E. C., Kim, S., and Walsh, C. A. (2006) *J. Neurosci.* **26,** 1767–1775
8. Assadi, A. H., Zhang, G., Beffert, U., McNeil, R. S., Renfro, A. L., Niu, S., Quattrocchi, C. C., Antalffy, B. A., Sheldon, M., Armstrong, D. D., Wynshaw-Boris, A., Herz, J., D'Arcangelo, G., and Clark, G. D. (2003) *Nat. Genet.* **35,** 270–276
9. Pramatarova, A., Ochalski, P. G., Chen, K., Gropman, A., Myers, S., Min, K. T., and Howell, B. W. (2003) *Mol. Cell. Biol.* **23,** 7210–7221
10. Jossin, Y., and Goffinet, A. M. (2007) *Mol. Cell. Biol.* **27,** 7113–7124
11. Strasser, V., Fasching, D., Hauser, C., Mayer, H., Bock, H. H., Hiesberger, T., Herz, J., Weeber, E. J., Sweatt, J. D., Pramatarova, A., Howell, B., Schneider, W. J., and Nimpf, J. (2004) *Mol. Cell. Biol.* **24,** 1378–1386
12. Jossin, Y., Ignatova, N., Hiesberger, T., Herz, J., Lambert de Rouvroit, C., and Goffinet, A. M. (2004) *J. Neurosci.* **24,** 514–521
13. Blake, S. M., Strasser, V., Andrade, N., Duit, S., Hofbauer, R., Schneider, W. J., and Nimpf, J. (2008) *EMBO J.* **27,** 3069–3080
14. Arnaud, L., Ballif, B. A., Förster, E., and Cooper, J. A. (2003) *Curr. Biol.* **13,** 9–17
15. Howell, B. W., Gertler, F. B., and Cooper, J. A. (1997) *EMBO J.* **16,** 121–132
16. Jossin, Y., Ogawa, M., Metin, C., Tissir, F., and Goffinet, A. M. (2003) *J. Neurosci.* **23,** 9953–9959
17. Kuo, G., Arnaud, L., Kronstad-O'Brien, P., and Cooper, J. A. (2005) *J. Neurosci.* **25,** 8578–8586
18. Howell, B. W., Lanier, L. M., Frank, R., Gertler, F. B., and Cooper, J. A. (1999) *Mol. Cell. Biol.* **19,** 5179–5188
19. Beffert, U., Durudas, A., Weeber, E. J., Stolt, P. C., Giehl, K. M., Sweatt, J. D., Hammer, R. E., and Herz, J. (2006) *J. Neurosci.* **26,** 2041–2052
20. Schneider, W. J., and Nimpf, J. (2003) *CMLS* **60,** 892–903
21. Gotthardt, M., Trommsdorff, M., Nevitt, M. F., Shelton, J., Richardson, J. A., Stockinger, W., Nimpf, J., and Herz, J. (2000) *J. Biol. Chem.* **275,** 25616–25624
22. Cuitino, L., Matute, R., Retamal, C., Bu, G., Inestrosa, N. C., and Marzolo, M. P. (2005) *Traffic* **6,** 820–838
23. Mayer, H., Duit, S., Hauser, C., Schneider, W. J., and Nimpf, J. (2006) *Mol. Cell. Biol.* **26,** 19–27
24. Riddell, D. R., Sun, X. M., Stannard, A. K., Soutar, A. K., and Owen, J. S. (2001) *J. Lipid Res.* **42,** 998–1002
25. Trommsdorff, M., Gotthardt, M., Hiesberger, T., Shelton, J., Stockinger, W., Nimpf, J., Hammer, R. E., Richardson, J. A., and Herz, J. (1999) *Cell* **97,** 689–701
26. Hack, I., Hellwig, S., Junghans, D., Brunne, B., Bock, H. H., Zhao, S., and Frotscher, M. (2007) *Development* **134,** 3883–3891
27. Brandes, C., Kahr, L., Stockinger, W., Hiesberger, T., Schneider, W. J., and Nimpf, J. (2001) *J. Biol. Chem.* **276,** 22160–22169
28. Koch, S., Strasser, V., Hauser, C., Fasching, D., Brandes, C., Bajari, T. M., Schneider, W. J., and Nimpf, J. (2002) *EMBO J.* **21,** 5996–6004
29. Stockinger, W., Hengstschläger-Ottnad, E., Novak, S., Matus, A., Hüttinger, M., Bauer, J., Lassmann, H., Schneider, W. J., and Nimpf, J. (1998) *J. Biol. Chem.* **273,** 32213–32221
30. Nandi, P. K., Irace, G., Van Jaarsveld, P. P., Lippoldt, R. E., and Edelhoch, H. (1982) *Proc. Natl. Acad. Sci. U.S.A.* **79,** 5881–5885
31. Rodal, S. K., Skretting, G., Garred, O., Vilhardt, F., van Deurs, B., and Sandvig, K. (1999) *Mol. Biol. Cell* **10,** 961–974
32. Howell, B. W., Herrick, T. M., Hildebrand, J. D., Zhang, Y., and Cooper,

J. A. (2000) *Curr. Biol.* **10,** 877–885
33. Hoe, H. S., and Rebeck, G. W. (2005) *Brain Res. Mol. Brain Res.* **137,** 31–39
34. May, P., Bock, H. H., Nimpf, J., and Herz, J. (2003) *J. Biol. Chem.* **278,** 37386–37392
35. Perez-Garcia, C. G., Tissir, F., Goffinet, A. M., and Meyer, G. (2004) *Eur. J. Neurosci.* **20,** 2827–2832
36. Beffert, U., Weeber, E. J., Durudas, A., Qiu, S., Masiulis, I., Sweatt, J. D., Li, W. P., Adelmann, G., Frotscher, M., Hammer, R. E., and Herz, J. (2005) *Neuron* **47,** 567–579
37. Beffert, U., Nematollah Farsian, F., Masiulis, I., Hammer, R. E., Yoon, S. O., Giehl, K. M., and Herz, J. (2006) *Curr. Biol.* **16,** 2446–2452
38. Burk, R. F., Hill, K. E., Olson, G. E., Weeber, E. J., Motley, A. K., Winfrey, V. P., and Austin, L. M. (2007) *J. Neurosci.* **27,** 6207–6211
39. Masiulis, I., Quill, T. A., Burk, R. F., and Herz, J. (2009) *Biol. Chem.* **390,** 67–73
40. Brandes, C., Novak, S., Stockinger, W., Herz, J., Schneider, W. J., and Nimpf, J. (1997) *Genomics* **42,** 185–191
41. Stockinger, W., Brandes, C., Fasching, D., Hermann, M., Gotthardt, M., Herz, J., Schneider, W. J., and Nimpf, J. (2000) *J. Biol. Chem.* **275,** 25625–25632
42. Bujo, H., Hermann, M., Kaderli, M. O., Jacobsen, L., Sugawara, S., Nimpf, J., Yamamoto, T., and Schneider, W. J. (1994) *EMBO J.* **13,** 5165–5175
43. Li, Y., Lu, W., Marzolo, M. P., and Bu, G. (2001) *J. Biol. Chem.* **276,** 18000–18006
44. Jossin, Y., Gui, L., and Goffinet, A. M. (2007) *J. Neurosci.* **27,** 4243–4252
45. Novak, S., Hiesberger, T., Schneider, W. J., and Nimpf, J. (1996) *J. Biol. Chem.* **271,** 11732–11736
46. Yamabhai, M., and Anderson, R. G. (2002) *J. Biol. Chem.* **277,** 24843–24846
47. Utsunomiya-Tate, N., Kubo, K., Tate, S., Kainosho, M., Katayama, E., Nakajima, K., and Mikoshiba, K. (2000) *Proc. Natl. Acad. Sci. U.S.A.* **97,** 9729–9734
48. Pol, A., Lu, A., Pons, M., Peiró, S., and Enrich, C. (2000) *J. Biol. Chem.* **275,** 30566–30572
49. Davis, C. G., Goldstein, J. L., Südhof, T. C., Anderson, R. G., Russell, D. W., and Brown, M. S. (1987) *Nature* **326,** 760–765
50. Cheng, H., Vetrivel, K. S., Drisdel, R. C., Meckler, X., Gong, P., Leem, J. Y., Li, T., Carter, M., Chen, Y., Nguyen, P., Iwatsubo, T., Tomita, T., Wong, P. C., Green, W. N., Kounnas, M. Z., and Thinakaran, G. (2009) *J. Biol. Chem.* **284,** 1373–1384
51. Vetrivel, K. S., Cheng, H., Lin, W., Sakurai, T., Li, T., Nukina, N., Wong, P. C., Xu, H., and Thinakaran, G. (2004) *J. Biol. Chem.* **279,** 44945–44954
52. Feng, L., Allen, N. S., Simo, S., and Cooper, J. A. (2007) *Genes Dev.* **21,** 2717–2730